

Nonlinear analysis of an RC frame structure considering the effects of embedment on soil–structure interaction

Nikola Petrov^{1,2}✉, Julijana Bojadjeva² and Jordan Bojadjev³

¹ Project Engineering, Jurij Gagarin, 31b-Local 1, 1000, Skopje, North Macedonia

² Ss Cyril and Methodius University, Institute of Earthquake Engineering and Engineering Seismology, Todor Aleksandrov, 165, 1000, Skopje, North Macedonia

³ International Balkan University, Faculty of Engineering, Civil Engineering, Makedonsko Kosovska Brigada, 1000, Skopje, North Macedonia

Corresponding author:
 Nikola Petrov

Received:
 February 13, 2025

Revised:
 June 12, 2025

Accepted:
 September 29, 2025

Published:
 December 3, 2025

Citation:
 Petrov, N.; Bojadjeva, J.;
 Bojadjev, J.
 Nonlinear analysis of an RC frame
 structure considering the effects of
 embedment on soil–structure
 interaction.

*Advances in Civil and
 Architectural Engineering*,
 2025, 16 (31), pp. 235-251.
<https://doi.org/10.13167/2025.31.14>

**ADVANCES IN CIVIL AND
 ARCHITECTURAL ENGINEERING
 (ISSN 2975-3848)**

Faculty of Civil Engineering and
 Architecture Osijek
 Josip Juraj Strossmayer University
 of Osijek
 Vladimira Preloga 3
 31000 Osijek
 CROATIA



Abstract:

The interaction between soil and structure, which merges geotechnical and structural engineering, plays a crucial role in seismic regions. Traditional structural design often assumes that buildings are fixed at their foundations, neglecting the influence of local soil conditions. However, accounting for soil–structure interaction (SSI) indicates greater structural flexibility, modified dynamic behaviour, and variations in the intensity and distribution of earthquake forces. These influences are especially notable in soft or moderately stiff soils, where foundation flexibility may cause increases or decreases in seismic demand. To account for these influences, American pre-codes provide detailed guidelines for incorporating SSI into structural analyses. In this study, these guidelines were applied in both nonlinear static (push-over) and nonlinear dynamic (time-history) analyses of a six-storey reinforced concrete frame structure. The analyses considered two different soil types, B and C, which were classified according to Eurocode 8, to evaluate the effect of different soil rigidity on structural behaviour. The findings, with a focus on kinematic interaction, highlighted how foundation embedment influences seismic behaviour. The results showed notable deformations in storey displacements and inter-storey drifts, as well as the formation of plastic hinges, indicating nonlinear response mechanisms. Reduced capacity curves under lower seismic forces confirmed the influence of SSI. This study underscores the necessity of incorporating SSI effects to improve seismic design accuracy and enhance the prediction of structural behaviour during earthquakes.

Keywords:

soil–structure interaction; kinematic interaction; period lengthening; push-over analysis; time-history analysis

1 Introduction

Soil–structure interaction (SSI) is a critical aspect of earthquake engineering that significantly influences the seismic responses of structures. This interaction involves a complex interplay between the structure, foundation, and surrounding soil, where these components affect the behaviour of the others during seismic events. Traditional design methods often assume fixed-base conditions and neglect the presence of soil. However, this simplification can lead to inaccurate predictions of the structural performance, particularly for buildings founded on soft soils or in regions with high seismic activity. This study explores the principles and implications of SSI, highlighting its impact on the dynamic characteristics and seismic response of structures.

SSI examines the total behaviour of the described coupled system when subjected to earthquakes [1-6]. EC 8 – 5, in Chapter 6 and Appendix D [7], outlines the influence of SSI on structural behaviour. It explains which categories of buildings and soil conditions are strongly impacted by this interaction, and describes its effects on the dynamic properties of the system. Nevertheless, it provides limited attention to how foundation configuration and the depth of structural embedment modify the response. This gap appears in most design codes, as highlighted by several studies in this area [8-11].

Unlike Eurocode 8, U.S. studies and pre-standard recommendations investigate this topic in greater depth. The NIST publication Soil-Structure Interaction for Building Structures [12] and FEMA P-2019 – Practical Guide for Soil-Structure Interaction [13] provide comprehensive guidance for incorporating soil characteristics into analyses and evaluating their effects on structural behaviour. Based on American studies and regulations, a preliminary criterion for estimating the significance of SSI is formulated as:

$$\frac{h'}{v_s \cdot T} \quad (1)$$

Where h' is the effective height of the structure; v_s is the shear-wave velocity, and T is the natural period of oscillation.

Values exceeding 0,1 [13] suggest a considerable potential for SSI to affect the structural response.

Based on this, it can be concluded that SSI's effect on structural behaviour depends not only on soil characteristics but also on the building height and its natural vibration period. Considering the thorough investigation of this topic in U.S. pre-codes and guidelines, this study applied quantitative recommendations to model and analyse a structural system founded on soil types B and C as per EC8. This approach was undertaken to assess how soil conditions affect structural behaviour and to emphasize the significance of including these factors in design. The goal was to evaluate structural systems thoroughly and realistically, preventing possible adverse outcomes if such effects are neglected. SSI alters the spectral acceleration intensity through both kinematic and inertial effects. Kinematic SSI arises from the presence of the structure as a geometric constraint within the soil, which modifies the transmitted acceleration. On the other hand, inertial SSI considers the structure's mass, which affects the inertial forces generated in response to ground acceleration. Particular focus is placed on the kinematic interaction between soil and structure, in order to examine how the foundation and depth of embedment affect structural behaviour.

This study examines the structural behaviour under seismic loading across various soil types and foundation embedment scenarios, while keeping the structural system unchanged. Nonlinear analysis techniques were employed to assess the behaviour of the structure. Specifically, nonlinear static (push-over) and dynamic (time-history) analyses were conducted. The nonlinear static analysis aimed to determine the failure mechanism of the structural system under different embedding and soil conditions as well as its capacity curves. The aim of the nonlinear dynamic analysis was to obtain the maximum displacement at the top of the structure. This analysis highlighted how different embedding and soil conditions modify seismic excitation and cause greater deformation when soil with lower stiffness is used. The structural

behaviour was assessed by analysing the storey displacements, inter-storey drifts, intensity of seismic force and its distribution, distribution of nonlinear deformations, and capacity curves. The influence of different soil types and foundation embedment scenarios on the structural response was carefully examined and is presented in this paper.

2 Analyses and effects of SSI

According to the literature [13; 14], two primary methods exist for representing the interaction between the structure, foundation, and soil: the substructure method and the direct method. In the first method, the soil is modelled using spring elements [13-15], and their stiffness characteristics are defined to simulate the behaviour of the soil. The springs can be assigned at the base of the foundation or along the walls of embedded structures to represent the soil's impact on the structure. To account for kinematic SSI effects within this approach, amplification factors are derived for every degree of freedom according to the soil characteristics. These factors are then used to modify the initial spring stiffness, resulting in an enhanced stiffness that captures the influence of kinematic SSI.

Conversely, the direct approach uses FE method [16; 17] to model the entire coupled system, providing a more precise simulation by extending the soil model adequately. Seismic forces are applied through these models to study the behaviour of a structure under seismic excitation. Whereas the first approach is commonly applied in design practice, the second one is used mostly for crucial buildings including nuclear facilities and large-scale infrastructure [18-20] (Figure 1).

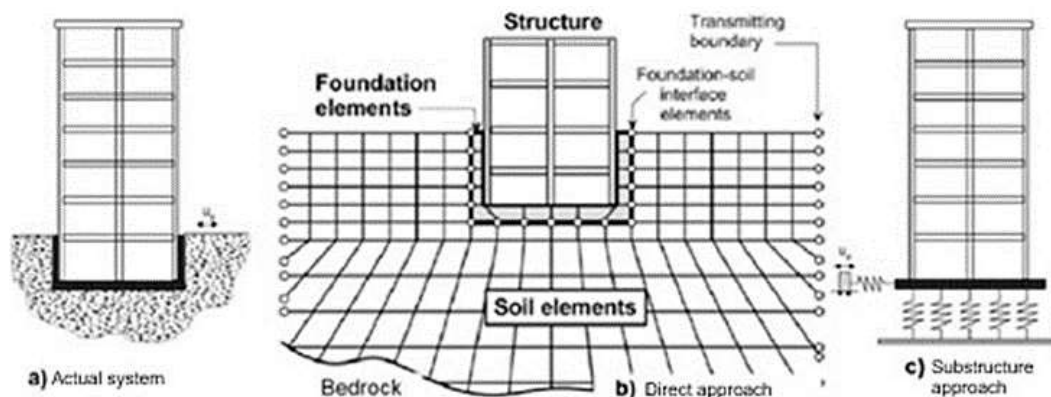


Figure 1. Methods for SSI modelling [12-13]

For this study, the substructure approach was incorporated into the analysis because it is more convenient and provides data with sufficient accuracy.

In this study, two analyses were conducted: a nonlinear static analysis to obtain the capacity curves and failure mechanism of the structure, and a nonlinear dynamic analysis using the acceleration time history ($\max a_g = 0,32 \text{ g}$) from El Centro earthquake data to determine the maximum displacements at the top of the structure under varying conditions, and the propagation of nonlinearities. The substructure method was employed to assess the effects of soil–structure interaction.

SSI effects cause the effective ground displacement at the spring ends to differ from the actual displacement near the foundation owing to the influence of the structure and soil deformation [21]. Energy dissipation through soil deformation manifests as kinematic and inertial interaction effects [22-24].

Kinematic interactions include base-slab averaging and embedment effects. Base-slab averaging refers to the spatial averaging of seismic motions across the foundation footprint, in which incoherent seismic wave propagation causes variations in motion across different parts of the foundation. This averaging effect typically reduces the effective input motion

experienced by the structure. In addition, deeper embedment tends to reduce the ground motion intensity because of the filtering and damping effects of the surrounding soil [12; 13; 25]. Inertial interactions include period lengthening, foundation damping, radial damping, and soil damping. Period elongation (Figure 2) happens as foundation flexibility rises, altering the structure's natural period and influencing the spectral acceleration values [12; 13; 26; 27].

In this context, the effect of period lengthening owing to SSI depends on where the fixed-base period falls on the response spectrum. Depending on this location, period lengthening may lead to an increase or reduction in spectral acceleration, and thus, influence the base shear intensity accordingly.

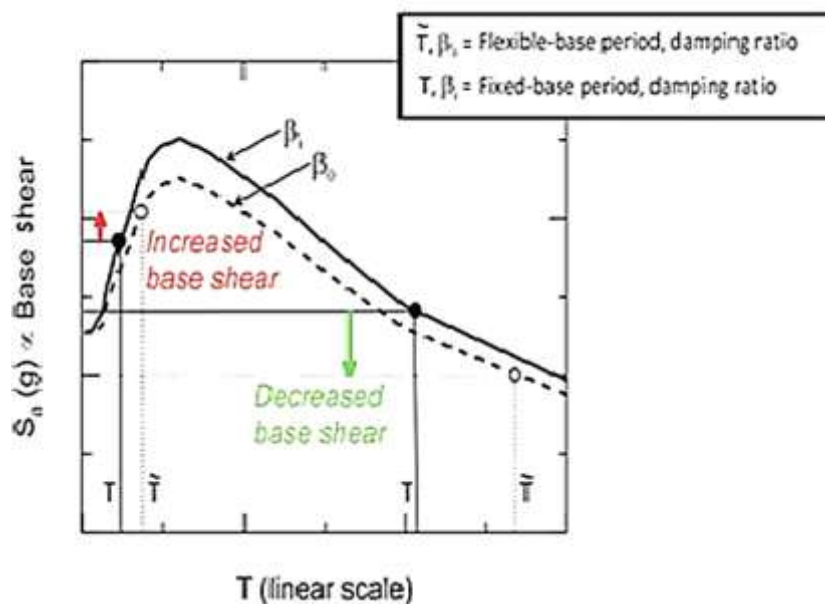


Figure 2. Period lengthening owing to SSI [13]

Vertical spring elements influence the foundation stiffness and rotation under seismic loads. Their stiffness is calculated using methods based on foundation and soil flexibility [12], as follows:

- Method 1 – rigid foundation and flexible soil;
- Method 2 – flexible foundation and nonlinear flexible soil; and
- Method 3 – flexible foundation and linear flexible soil.

In this study, Method 1 was used to modify the stiffness values of uniformly distributed springs under the foundation slab. ASCE/SEI 41-17 [15] provides the equations for calculating these characteristics for every degree of freedom. The rigidity of the spring components and correction coefficients for embedding were calculated according to Pais and Kausel (1988) [28].

3 Case study

The building examined in the study (Figure 3) was a RC frame structure [29; 30] featuring a basement, ground floor, and four additional floors (B+GF+4). This structural system was selected because it is representative and the most prevalent in the region of interest. The dimensions at the basement and ground floor levels were 27,00 × 26,00 m, whereas the upper floors measured 17,00 × 16,00 m. Each floor had a height of 3 m. The building was symmetrical along the X- and Y-axes. The spans in the X-direction were 5-6-5-6-5 m, and those in the Y-direction were 5-6-4-6-5 m. All columns were 50 × 50 cm, except for those in the central part of the building, which were 60 × 60 cm. The beams' cross-sections are 35 × 50 cm and the slabs have thickness of 16 cm.

The basement is completely embedded in the soil, featuring 20cm thick reinforced concrete walls along its perimeter, reaching the full height of the floor. The foundation consisted of an 80-cm-thick reinforced concrete slab. The sizes of the structural elements were determined following PBAB '87 [31] and PIOVS '81 [32], which have been the standard design norms for buildings in the country over the past decades. While the adoption of Eurocodes has been gradually increasing in recent years, the transition remains slow, and the simultaneous use of PBAB '87, PIOVS '81, and Eurocodes is still permitted.

Nonlinear analyses were conducted by use of the computer software CSI ETABS 20 [33]. The nonlinear static analysis was performed until a structural element failed, yielding the capacity curves and failure mechanism of the structure. A nonlinear dynamic analysis was also conducted using the acceleration time history from the El Centro earthquake, with a maximum $a_g = 0,32$ g, representing the maximum expected earthquake at a hypothetical location. This analysis provided displacement–time histories for the top of the structure, highlighting the impact of various embedding and soil conditions on the excitation and structural response.

For the purposes of this paper, few versions (Figure 4) of the described model were examined:

- Model 1 – fixed-base model; and
- Model 2 – model with foundation, vertical spring elements (V) below the foundation slab, and horizontal spring elements (H) on the basement walls.

Additionally, for Model 2, the /B or /C designation was included to indicate the soil type considered in the analysis. Thus, the following models were generated:

- Model 2/B, analysed for soil type B, characterised by medium-dense to dense soil conditions with moderate shear wave velocities; and
- Model 2/C, analysed for soil type C, which typically consists of soft soil with lower shear wave velocities and higher deformability.

As indicated previously, a variant of a rigid foundation structure in flexible soil was considered [12; 15; 28].

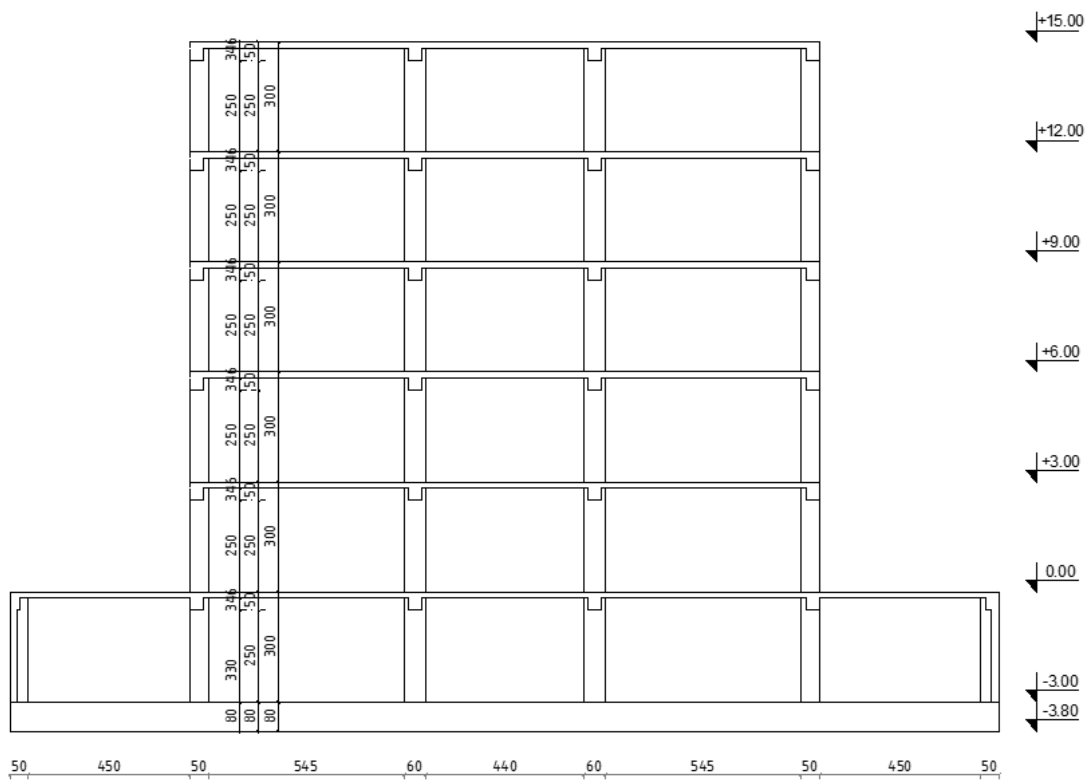


Figure 3. Elevation view of the case study structure

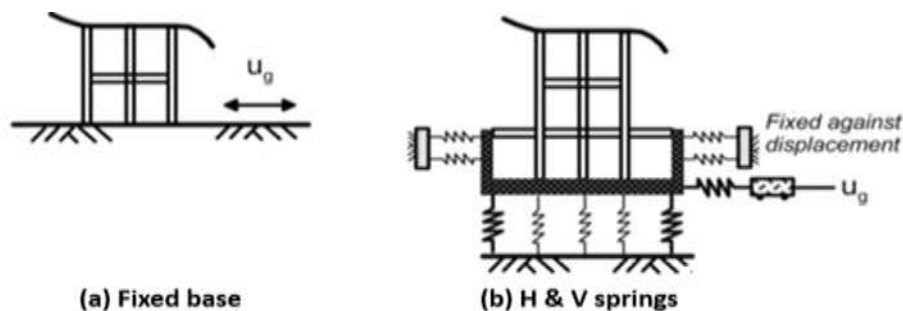


Figure 4. Model variants: a) Model 1, and b) Model 2 [12]

4 Calculation of stiffness characteristics of springs

Based on the equations for evaluating the rigidity of the springs [28] for all three translational and rotational directions, together with the formulas for calculating coefficients related to embedding effects, computations were carried out for soil types B and C [29; 30; 34] in accordance with Eurocode 8. Although SSI effects may be notable for soil type D, this type was excluded from the study as it does not occur in the area of interest and is therefore outside the scope of the analysis. Similarly, SSI can affect structures founded on highly competent soils (soil type A). However, this type was not considered in the study because it is expected to provide nearly full foundation stiffness. Consequently, no significant translation or rotation of the foundation is anticipated, resulting in minimal changes in seismic force magnitudes and bending moments compared with a fixed-base model. The values for the shear wave velocity (V_s) and effective shear modulus (G), which were the primary parameters in the calculations, were hypothetically selected to demonstrate how varying soil parameters affect SSI. A 3,0 m embedment depth was chosen, as it reflects the typical depth at which buildings are commonly founded in the study area.

4.1 Soil type B

For soil type B, the soil was theoretically assumed to have the following properties: $V_s = 400$ m/s and $G = 70000$ kN/m². The embedment depth was $e = 3,00$ m. Using these input parameters, the spring properties and the correction factor accounting for embedment effects were computed. The resulting values are presented in Table 1. The Z-axis was perpendicular to the plane of the foundation/basement wall.

Table 1. Stiffness and correction coefficients of springs – soil type B [28]

Degree of freedom	Spring stiffness ($\frac{kN}{m} / \frac{kN/m}{rad}$)	Correction coefficient owing to embedding
translation in Z-direction	6.225.700,00	1,32
translation in Y-direction	5.031.574,00	1,53
translation in X-direction	5.015.104,00	1,53
rotation around Z-axis	1.341.312.106,00	2,64
rotation around Y-axis	956.491.364,00	1,29
rotation around X-axis	905.840.000,00	1,29

4.2 Soil type C

The same calculations were carried out for soil type C, with the following characteristics considered, i.e., $V_s = 250$ m/s and $G = 14000$ kN/m². The embedment depth was $e = 3,00$ m. Using these input parameters, the spring properties and the correction factor accounting for embedment effects were computed. The resulting values are presented in Table 2. The Z-axis was perpendicular to the plane of the foundation/basement wall.

Table 2. Stiffness and correction coefficients of springs – soil type C [28]

Degree of freedom	Spring stiffness ($\frac{kN}{m}$ / $\frac{kN/m}{rad}$)	Correction coefficient owing to embedding
translation in Z-direction	1.245.140,00	1,32
translation in Y-direction	1.006.315,00	1,53
translation in X-direction	1.003.021,00	1,53
rotation around Z-axis	268.262.421,00	2,64
rotation around Y-axis	191.298.273,00	1,29
rotation around X-axis	181.168.000,00	1,29

5 Nonlinear analysis

5.1 Basic concept

Nonlinear analyses were first used for research purposes in the 1970s. Their accuracy stems from the fact that the stiffness of the system changes under the action of an applied force, resulting in a nonlinear relationship between the applied stress on the system and its strains (Figure 5) caused by geometric, material, or joint nonlinearities.

Nonlinear analyses have found widespread application in earthquake engineering and the seismic design of ductile structural systems capable of withstanding extreme earthquakes. Numerous computer programs have been developed for the nonlinear analysis of structures, enabling faster and easier implementation.

There are two main types of nonlinear analysis:

- nonlinear static analysis, known as push-over analysis;
- nonlinear dynamic analysis, known as time-history analysis.

These methods are central to performance-based design (PBD), which shifts the focus from prescriptive code compliance to evaluating the performance of a structure under various levels of seismic demand. The essence of PBD is to ensure that a structure meets predefined performance objectives, —such as immediate occupancy, life safety, and collapse prevention, under different earthquake intensities [35-42].

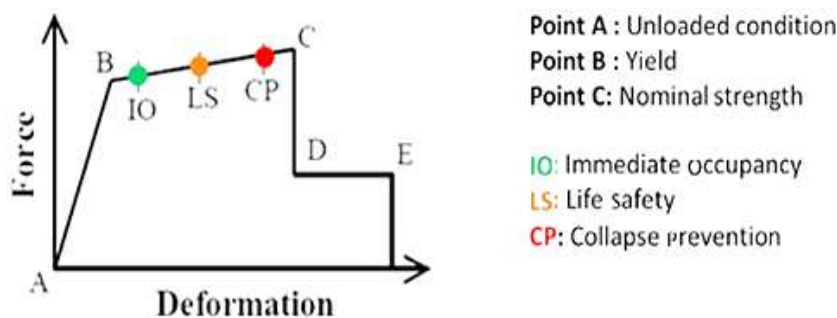


Figure 5. Force–deformation relationship for PBD

5.2 Models for nonlinear analysis

Models for nonlinear analysis were employed based on the design of the structural members with dimensions and reinforcement details [29]. This entailed defining the nonlinear characteristics of the materials used in the model (concrete MB30 and reinforcement RA 400/500-2), as shown in Figure 6, and the geometric nonlinearity of the structural elements expressed through the moment–curvature and moment–rotation relationships at the beam sections (Figure 7). In addition, the moment–curvature, moment–rotation, and moment–axial force relationships of the columns were considered (Figure 8). Given that the behaviour of the

columns largely depends on the magnitude of the axial force acting on them, the moment–curvature/moment–rotation diagrams for the columns were analysed for three different levels of axial force. Nonlinear static and dynamic analyses were conducted on Models 1, 2/B, and 2/C using the computer program ETABS [33]. The spring elements were assigned stiffness values that were adjusted using correction factors, as defined in Tables 1 and 2, to account for kinematic SSI effects. These corrected stiffnesses were uniformly distributed across the foundation area and basement walls through the spring elements implemented in the analysis software [12]. The plastic hinges of the structural elements were automatically defined using the computer program, with M3 plastic hinges specified at each end of the beams, as well as P-M2-M3 plastic hinges at the base and top of each column, as shown in Figure 9 [11; 37]. In this context, P refers to the axial force, M2 denotes the bending moment about the local 2-axis (typically the minor axis), and M3 represents the bending moment about the local 3-axis (usually the major axis). Thus, the P-M2-M3 hinges captured the combined axial and biaxial bending behaviour of the columns, while the M3 hinges represented the flexural behaviour at the ends of the beams. Analyses of the obtained results were performed to evaluate the structural response to horizontal forces from the maximum expected earthquake (dynamic time-history analysis) and up to the ultimate limit state of a structural member (static push-over analysis).

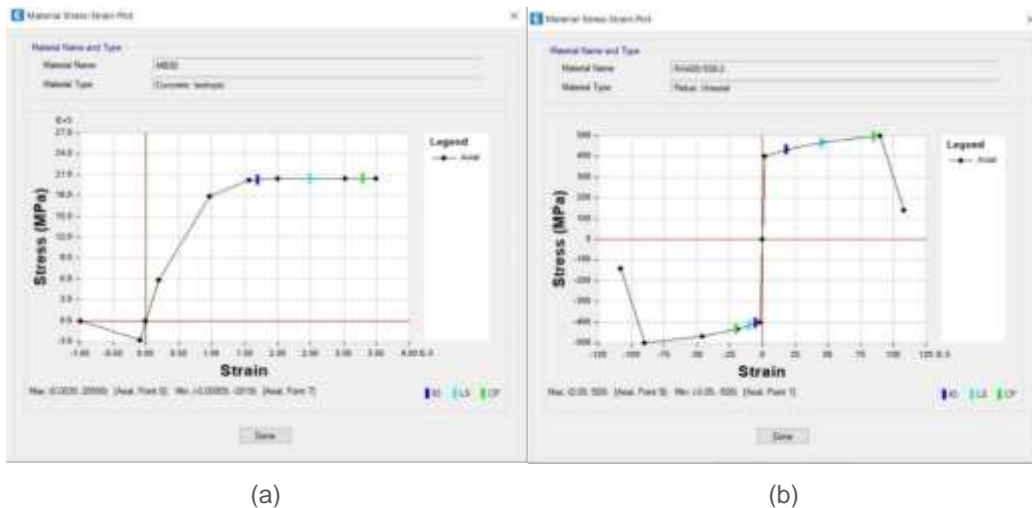


Figure 6. Stress–strain relationship: a) concrete MB30, and b) rebar RA400/500-2 [33]

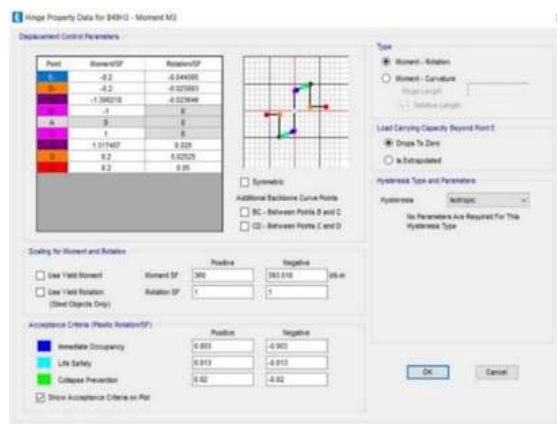


Figure 7. Definition of plastic hinges in beam on first storey: moment–rotation diagram [33]

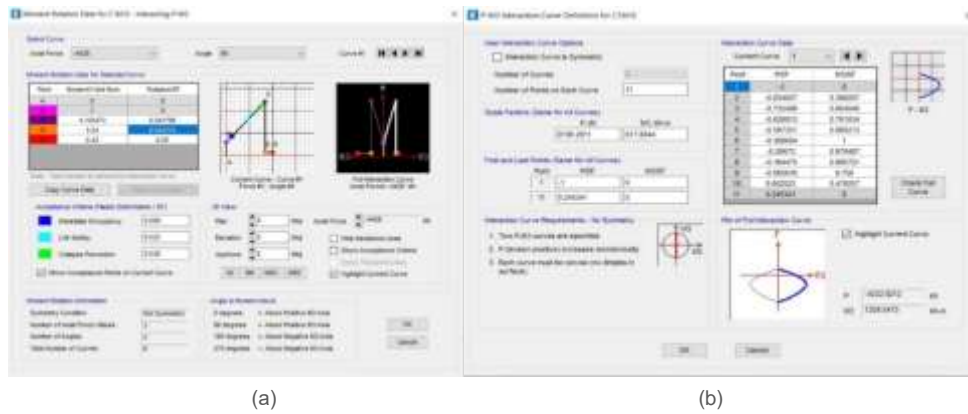


Figure 8. Definition of plastic hinges in column on first storey: a) moment–rotation diagram, and b) moment–axial force diagram [33]

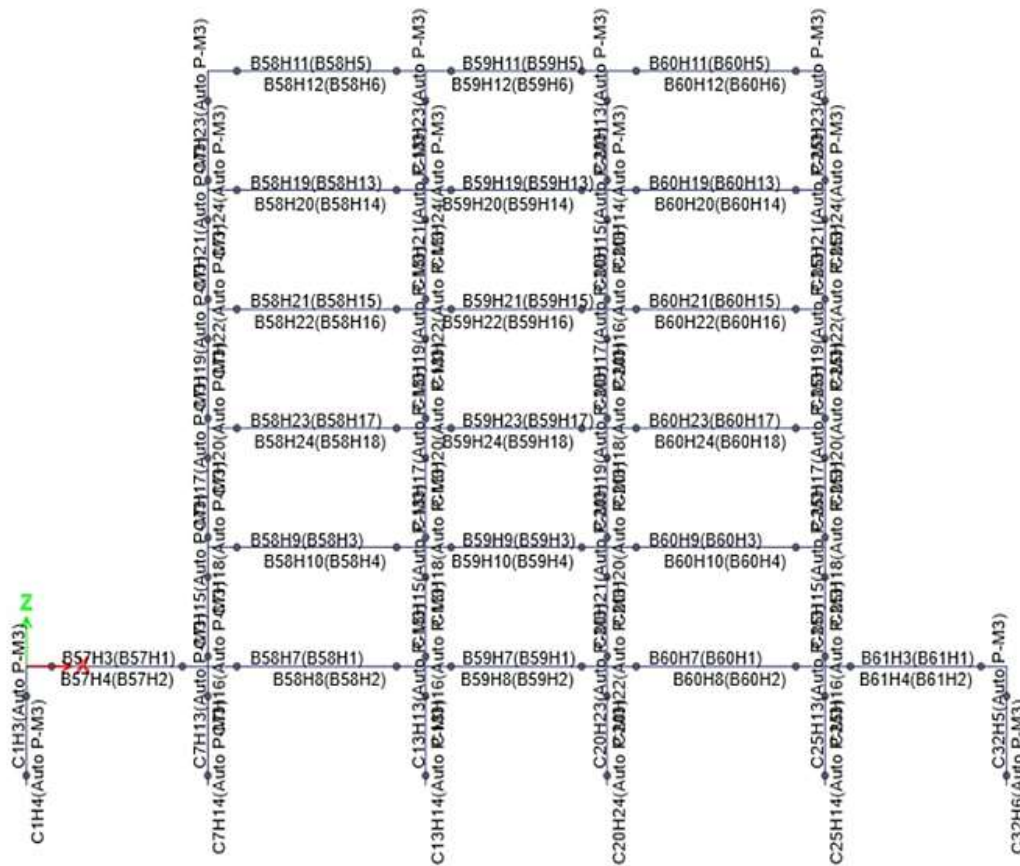


Figure 9. Plastic hinge disposition (frame Rx2) [33]

5.3 Nonlinear static (push-over) analysis

A nonlinear static analysis was conducted on the proposed models to obtain the structural capacity under different soil and embedding conditions. From the executed nonlinear static analysis, it can be observed that the behaviours of Models 1 and 2/B were similar in terms of the distribution of deformations, as well as the overall displacement at the top and inter-storey displacements (Figure 10). This is primarily a result of the favourable characteristics of soil type B. The difference is noticeable in the magnitude of the horizontal force under which the specified deformations occurred in Model 2/B compared with Model 1. It had a lower intensity,

indicating that the capacity of the structure with the included soil conditions for soil type B was lower than that of the model with a fixed base. The maximum displacement at the top of the structure in Model 2/B was 3,70 % greater than that in Model 1.

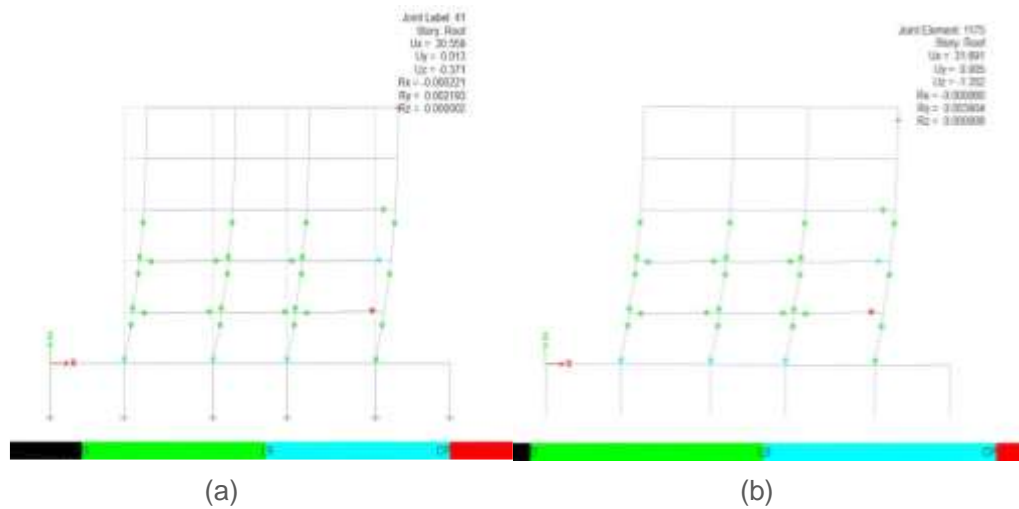


Figure 10. Final step of push-over analysis: a) Model 1 and b) Model 2/B [33]

In contrast to Model 2/B, Model 2/C, located on soil type C, exhibited significantly larger displacements at the top of the structure, as well as inter-storey displacements of greater magnitude. The maximum displacement at the top in Model 2/C was 20,58 % greater than that in Model 1 (Figure 11). There was also noticeable displacement at the foundation, indicating that unfavourable soil conditions not only reduce the capacity of the structure but also significantly influence its behaviour in the case of an earthquake, which, without control, can often exceed the prescribed limits.

The first failure in the fixed-base model occurred at a total horizontal force at the base of 29.270,20 kN, which corresponded to 94,86 % of the seismic weight of the structure. In contrast, the models founded on soil types B and C experienced their first failure at significantly lower horizontal forces of 19.422,13 kN (62,94 % of the seismic weight) and 19.979,86 kN (60,55 % of the seismic weight), respectively. This demonstrates that SSI has a pronounced effect on the lateral capacity of the structure, with the impact being more significant for softer soils (type C), where the interaction reduces the resistance of the structure to seismic forces.

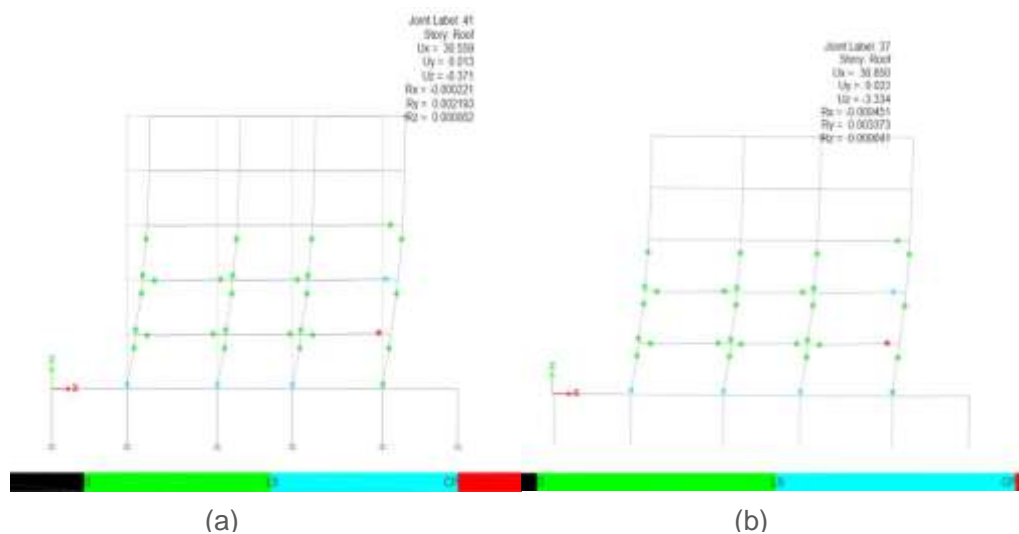


Figure 11. Final step of push-over analysis: a) Model 1, and b) Model 2/C [33]

In all cases, the collapse in the final step of the analysis occurred in a beam on the first storey (level +3,00 m). This demonstrates that the weak beam–strong column rule for capacity design is respected. By ensuring that the beams yield before the columns, the structure can better dissipate energy and maintain its stability during seismic events. This design principle helps to prevent catastrophic failures by localising the damage to the beams, thereby allowing the columns to continue supporting the structure. Consequently, the overall safety and resilience of the building are significantly enhanced. The obtained results are graphically shown in Figures 12, 13 and 14. The nonlinear static analysis results clearly indicated the influence of SSI on the seismic response of the models. Structures under softer soil conditions (soil type C) exhibited a significantly lower base shear capacity and larger top displacements than those under stiffer soil (soil type B) and fixed-base conditions (Model 1), as shown in the capacity curves and displacement diagrams. The increased flexibility introduced by soil compliance led to amplified inter-storey drifts and displacements, highlighting the detrimental effect of SSI on structural performance. These results point to the critical importance of accounting for soil conditions in seismic design, as neglecting SSI may lead to an underestimation of structural demands, particularly for softer soil conditions.

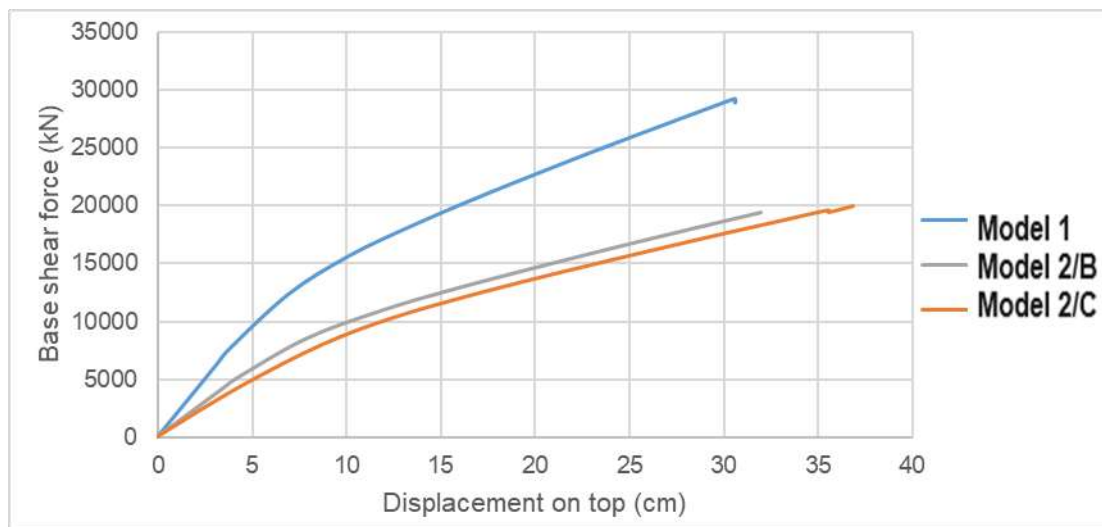


Figure 12. Capacity curves

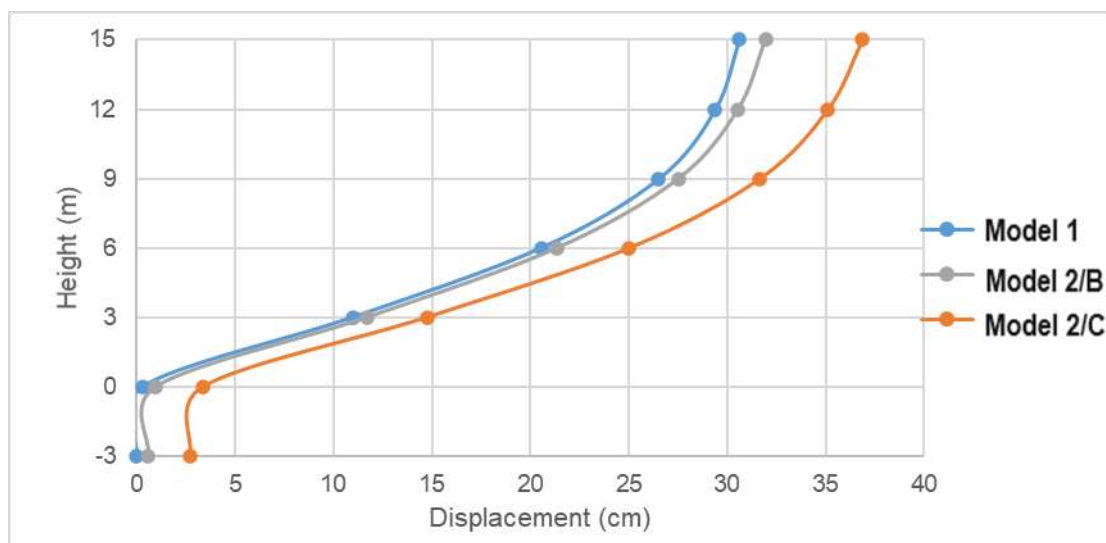


Figure 13. Storey displacements

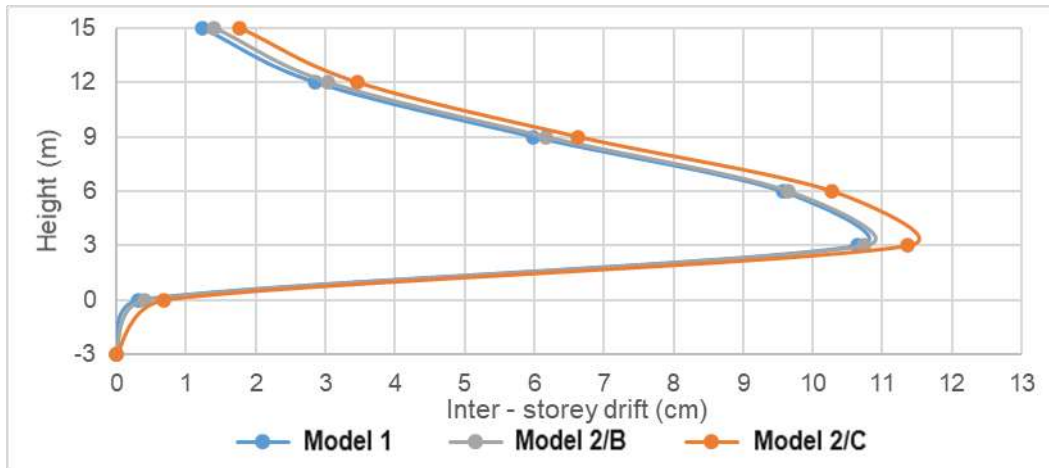


Figure 14. Inter-storey drifts

5.4 Nonlinear dynamic (time-history) analysis

Nonlinear dynamic analysis is performed using records of actual earthquake events (time histories) or, in specific cases, artificially generated events where the intensity of the ground motion is applied to a structural model. The purpose is to calculate the deformations of each element of the structural system for every degree of freedom [42-46].

A nonlinear dynamic analysis of an earthquake record from El Centro was conducted using Models 1, 2/B, and 2/C. According to the hypothetical location of the structure, for the maximum expected earthquake, the maximum acceleration was 0,32 g (Figure 15). The ground motion was scaled to obtain the maximum acceleration of 0,32 g. No additional modifications were made to the ground motion record, because the kinematic SSI effects were incorporated through the inclusion of spring elements in the models. The stiffness of these springs was adjusted using correction factors to account for kinematic SSI effects.

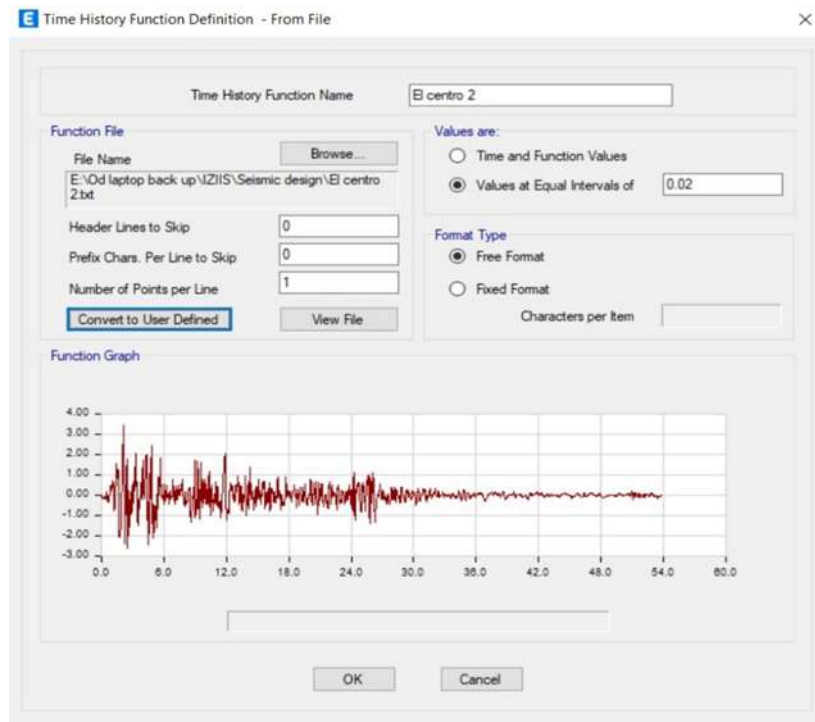


Figure 15. El Centro acceleration time-history data [33]

Following the analysis, the focus of the result processing was on the deformations, specifically the displacements of the top of the structure. In general, from the time histories of the displacements, nonlinear behaviour was evident in the models, along with differences in the maximum values at different time intervals. This variation arose from the dynamic characteristics of the structural models, which depended on the type of soil medium.

The analysis of the deformations indicated that the maximum displacements during the maximum earthquake exceeded the criterion of $H/600$ (where H represents the total height of the structure) according to linear analysis as per the national code [33]; however, there was no failure in the structural members.

From the results of the distribution of the plastic hinges at the end of the analysis, it could be observed that the yield limit was exceeded in almost all structural elements; however, all remained in the zone of initial nonlinearity (Figure 16).

The displacements at the top of the structure were the smallest for the model with a fixed base, amounting to 9,72 cm. In this case, it should be noted that at the end of the analysis, a large number of elements remained in the elastic zone, that is, the yield limit was not exceeded.

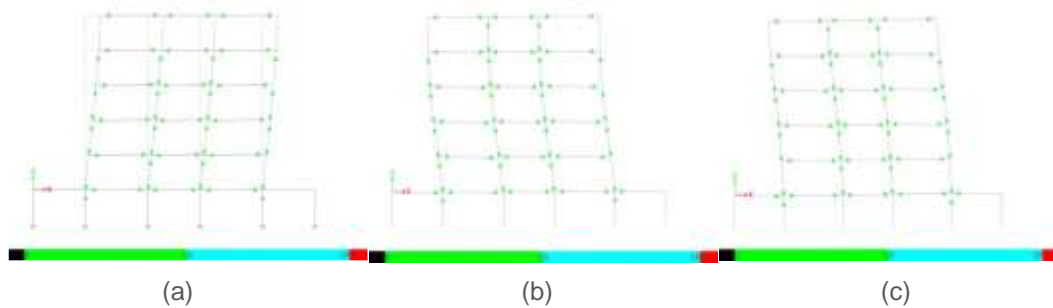


**Figure 16. Plastic hinge distribution at the end of the analysis – El Centro 0,32 g:
a) Model 1, b) Model 2/B, and c) Model 2/C**

For Models 2/B and 2/C, the maximum displacements at the top were 10,84 and 12,69 cm, respectively (Figure 17).

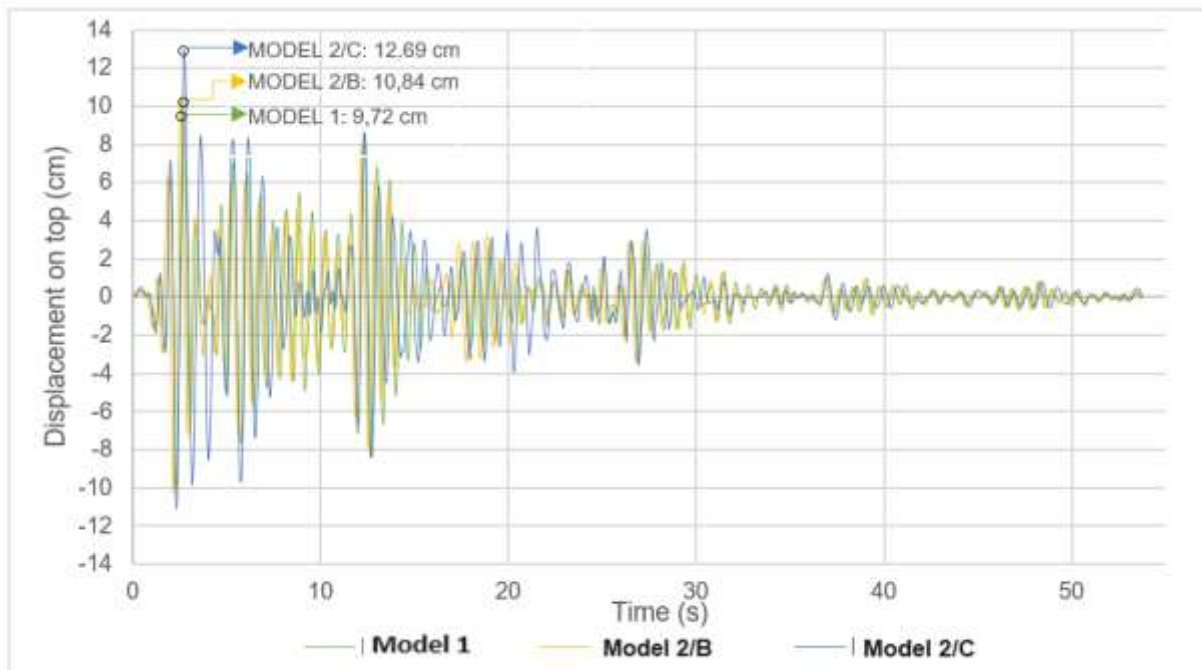


Figure 17. Time histories of top displacements

6 Conclusions

To assess the impact of SSI, including kinematic effects, mathematical models of an RC frame were developed following American standards and guidelines for representing soil conditions. The RC frame structure investigated in this study consisted of 6 storeys within plan and elevation regularity. Nonlinear static and dynamic analyses were performed on Model 1, Model 2/B, and Model 2/C by use of CSI ETABS computer software. Initially, following American guidelines, the stiffness properties of springs representing Eurocode 8 soil types B and C were determined. Subsequently, nonlinearities were applied to Models 1, 2/B, and 2/C. Material nonlinearity was expressed through the nonlinear behaviour of the steel and concrete, whereas geometrical nonlinearity was incorporated by defining and applying plastic hinges at each end of the beams and at the base and top of each column. The following conclusions were drawn from the nonlinear static push-over analysis:

- When the structure was founded on stiffer soil, almost identical distributions and levels of deformation for the plastic hinges occurred in the model that accounted for SSI effects, as in the fixed-base model. The difference lay in the intensity of the force at each subsequent level of deformation, which was lower when the local soil conditions were incorporated.
- In the case of softer soil, a uniform distribution of deformations in the structural elements occurred, which was most evident at the base of the ground-floor columns in the final phases of the analysis.
- The inclusion of local soil conditions significantly reduced the capacity of the structures.
- Translational displacements at the foundation level were observed by simulating the local soil conditions, proving that the soil serves as a form of base isolation that dissipates a portion of the seismic force.
- The maximum displacement at the top under an almost identical maximum horizontal force was 3,70% greater in the model founded on soil type B than in the fixed-base model, and 20,58% greater in the model based on soil type C than in the fixed-base model.
- Noticeable inter-storey drifts were observed for the model founded on soil type C.
- The results indicate that the first failure occurred at significantly lower base shear values for models in which local soil conditions were included in the analysis compared with the fixed-base model.
- The interaction was more pronounced in the case of softer soils (type C), where it notably reduced the ability of the structure to withstand lateral forces, making the structure more vulnerable to seismic events.
- The influence of SSI was less significant in stiffer soils (type B), where the structure retained a higher lateral capacity.

The nonlinear dynamic analysis led to the following conclusions:

- Including the local soil conditions altered the dynamic characteristics of the structures and influenced their behaviour during earthquakes.
- Unfavourable soil conditions led to the amplification of seismic forces, resulting in larger deformations.
- For the maximum expected earthquake, the yield limit was exceeded in almost all structural elements when the local soil conditions were incorporated, placing them in the zone of initial nonlinearity.
- The maximum displacements at the top of the structure exceed the prescribed value according to national regulations ($H/600$). However, deep nonlinearity or failure did not occur in any of the structural elements.
- Under the action of an earthquake of the same intensity, the maximum displacement at the top of the model founded on soil type B was 11,52 % greater than that in the fixed-base model, and for the model founded on soil type C, it was 30,55 % greater than the top displacement in the fixed-base model.

Based on the research and analyses conducted in this study, it is clear that a more detailed and comprehensive approach to SSI is necessary. In addition, the kinematic effects between soil and structures must be considered. Observations show that structures undergo different behaviours during earthquakes, even on favourable soils, compared with their responses when modelled with a fixed base. Hence, including local soil conditions in structural analysis is crucial, even for favourable soils, primarily because of kinematic interaction effects. This requirement differs from most standards, which usually require modelling local soil conditions only when weak-bearing soils are present.

Accounting for local soil conditions is crucial not only to capture variations in seismic force intensity but also, more importantly, to reflect the overall deformations the structure undergoes under these altered forces. Such deformations would not be properly represented if the structure was analysed with a fixed base.

This study, however, was limited to a specific structural type, seismic hazard, and soil properties, characterized by the shear modulus (G) and shear wave velocity (V_s). Therefore, it does not offer a comprehensive assessment of soil types B and C. Future research should examine different structural systems, including those with irregularities in plan and elevation.

References

- [1] Kraus, I.; Džakić, D.; Papić, J.; Cerovečki, A. Influence of foundation contact pressure on response spectrum-based design. *Građevinar*, 2020, 72 (1), pp. 11-20. <https://doi.org/10.14256/JCE.2365.2018>
- [2] Bačić, M.; Ivšić, T.; Kovačević, S. M. Geotechnics as an unavoidable segment of earthquake engineering. *Građevinar*, 2020, 72 (10), pp. 923-936. <https://doi.org/10.14256/JCE.2968.2020>
- [3] Borghei, A.; Ghayoomi, M. The role of kinematic interaction on measured seismic response of soil-foundation-structure systems. *Soil Dynamics and Earthquake Engineering*, 2019, 125, 105674. <https://doi.org/10.1016/j.soildyn.2019.05.013>
- [4] Lulayehu Tadesse, Z.; Padavala, H. K.; Koteswara, V. R. P. Effect of subterranean levels on the foundation input motions for dynamic response analysis of building structure. *Asian Journal of Civil Engineering*, 2023, 24, pp. 793-808. <https://doi.org/10.1007/s42107-022-00531-y>
- [5] Zogh, P.; Motamed, R.; Ryan, K. Empirical evaluation of kinematic soil-structure interaction effects in structures with large footprints and embedment depths. *Soil Dynamics and Earthquake Engineering*, 2021, 149, 106893. <https://doi.org/10.1016/j.soildyn.2021.106893>
- [6] Abdulaziz, M. A.; Hamood, M. J.; Fattah, M. Y. A review study on seismic behavior of individual and adjacent structures considering the soil – Structure interaction. *Structures*, 2023, 52, pp. 348-369. <https://doi.org/10.1016/j.istruc.2023.03.186>
- [7] European Committee for Standardization. *Eurocode 8: Design of structures for earthquake resistance – Part 5: Foundations, retaining structures and geotechnical aspects*. Brussels: CEN, 2004.
- [8] Bararnia, M. et al. Estimation of inelastic displacement ratios for soil-structure systems with embedded foundation considering kinematic and inertial interaction effects. *Engineering Structures*, 2018, 159, pp. 252-264. <https://doi.org/10.1016/j.engstruct.2018.01.002>
- [9] Asadi-Ghoozhdi, H.; Attarnejad, R. A Winkler-based model for inelastic response of soil–structure systems with embedded foundation considering kinematic and inertial interaction effects. *Structures*, 2020, 28, pp. 589-603. <https://doi.org/10.1016/j.istruc.2020.09.009>
- [10] Anand, V.; Satish Kumar, S. R. Soil-structure Interaction: A State-of-the-Art Review. *Structures*, 2018, 16, pp. 317-326. <https://doi.org/10.1016/j.istruc.2018.10.009>
- [11] Mekkiab M. et al. Soil-structure interaction effects on RC structures within a performance-based earthquake engineering framework. *European Journal of*

- Environmental and Civil Engineering*, 2014, 18 (8), pp. 945-962.
<https://doi.org/10.1080/19648189.2014.917056>
- [12] National Institute of Standards and Technology, U.S. Department of Commerce. NIST GCR 12-917-21 Soil-Structure Interaction for Building Structures. Accessed: November 19, 2025. Available at: <https://www.nehrp.gov/pdf/nistgcr12-917-21.pdf>
- [13] Federal Emergency Management Agency (FEMA), Applied Technology Council. A Practical Guide to Soil-Structure Interaction. Accessed: November 19, 2025. Available at: <https://www.fema.gov/sites/default/files/documents/fema-p-2091-soil-structure-interaction.pdf>
- [14] Dhehbiya, G.; Salah, K. Effects and dynamic behaviour of soil - framed structure interaction. *Građevinar*, 2022, 74 (1), pp. 9-20.
<https://doi.org/10.14256/JCE.2301.2017>
- [15] Sanghai S. S.; Pawade, P. Y. Effectiveness of friction dampers on seismic response of structure considering soil-structure interaction. *Građevinar*, 2020, 72 (1), pp. 33-44.
<https://doi.org/10.14256/JCE.1982.2017>
- [16] Edip, K. et al. Boundary effects in simulation of soil-structure interaction problems. *Soil Mechanics and Foundation Engineering*, 2017, 54 (4), pp. 239-243.
<https://doi.org/10.1007/s11204-017-9464-2>
- [17] Sheshov, V. Relevant aspects of applying soil improvement method for liquefaction mitigation – case study. In: *Fourth International Conference on Recent Advances in Geotechnical Earthquake Engineering and Soil Dynamics*, Talaganov, K. (ed.). March 26-31, 2001, San Diego, CA, USA. Missouri University of Science and Technology, 2001.
- [18] Petrov, N. Experimental and numerical methods in earthquake geotechnical engineering. [seminar work], Ss. Cyril and Methodius University, Institute of Earthquake Engineering and Engineering Seismology, Skopje, R. Macedonia, 2024.
- [19] Sheshov, V. Lecture Notes: Dynamic Soil-Structure Interaction. Skopje, R. Macedonia: Institute of Earthquake Engineering and Engineering Seismology, 2011.
- [20] Lou, M.; Huaifeng, W.; Xi, C.; Yongmei, Z. Structure–soil–structure interaction: Literature review. *Soil Dynamics and Earthquake Engineering*, 2011, 31 (12), pp. 1724-1731. <https://doi.org/10.1016/j.soildyn.2011.07.008>
- [21] American Society of Civil Engineers. ASCE/SEI. 41-17. *Seismic Evaluation and Retrofit of Existing Buildings*. USA: ASCE; 2017. <https://doi.org/10.1061/9780784412855>
- [22] Oliver, S.; Hare, J.; Harwood, N. Soil Structure Interaction Starts With Engineers. In: *NZSEE Conference*. April 26-28, 2013, Wellington, New Zealand, The New Zealand Society for Earthquake Engineering (NZSEE), 2013.
- [23] American Society of Civil Engineers. ASCE/SEI 7-16. *Minimum Design Loads and Associated Criteria for Buildings and Other Structures*. USA: ASCE; 2017.
<https://doi.org/10.1061/9780784414248>
- [24] Kim, S.; Stewart, J. P. Kinematic soil-structure interaction from strong motion recordings. *Journal of Geotechnical and Geoenvironmental Engineering*, 2003, 129 (4), pp. 323-335. [https://doi.org/10.1061/\(ASCE\)1090-0241\(2003\)129:4\(323\)](https://doi.org/10.1061/(ASCE)1090-0241(2003)129:4(323))
- [25] Thusoo, S. et al. Dynamic Soil Structure Interaction in Buildings. *International Journal of Civil and Environmental Engineering*, 2016, 10 (5), pp. 617-622.
- [26] Khalil, L.; Sadek, M.; Shahrour, I. Influence of the soil–structure interaction on the fundamental period of buildings. *Earthquake Engineering & Structural Dynamics*, 2007, 36 (15), pp. 2445-2453. <https://doi.org/10.1002/eqe.738>
- [27] Mercado, J. Study of Period Lengthening Effects in Soil–Structure Interaction Systems. In: *IFCEE 2021: Earth Retention, Ground Improvement, and Seepage Control*, El Mohtar, C. et al (eds.), USA: American Society of Civil Engineers; 2021.
<https://doi.org/10.1061/9780784483411>
- [28] Pais, A.; Kausel, E. Approximate formulas for dynamic stiffnesses of rigid foundations. *Soil Dynamics and Earthquake Engineering*, 1988, 7 (4), pp. 213-227.
[https://doi.org/10.1016/S0267-7261\(88\)80005-8](https://doi.org/10.1016/S0267-7261(88)80005-8)

- [29] Petrov N. Kinematic Soil – Structure interaction effects on seismic performance of RC frames. [master thesis], Ss. Cyril and Methodius, Institute of Earthquake Engineering and Engineering Seismology, Skopje, R. Macedonia, 2023.
- [30] Petrov, N.; Bojadjieva, J.; Bojadjiev, J. Kinematic SSI effects on seismic performance of RC structures. *Građevinar*, 2024, 76 (7), pp. 647-658. <https://doi.org/10.14256/JCE.3913.2023>
- [31] Sojuzen zavod za standardizacija. Pravilnik za tehnicki normative za beton i armiran beton. *Sluzben list na SFRJ*, 1987, 11, pp. 309-352. [in Macedonian]
- [32] Sojuzen zavod za standardizacija. Pravilnik za tehnicki normative za izgradba na objekti na visokogradba vo seizmicki podracja. *Sluzben list na SFRJ*, 1981, 31, pp. 844-854. [in Macedonian]
- [33] Computers and Structures, Inc. ETABS 20.0, Version 20.0. Accessed: November, 19, 2025. Available at: <https://www.csiamerica.com/products/etabs>
- [34] European Committee for Standardization. *Eurocode 8. Design of structures for earthquake resistance - Part 1: General rules, seismic actions and rules for buildings*. Brussels: CEN, 2004.
- [35] Mitrović, S.; Čaušević, M. Nonlinear static seismic analysis of structures. *Građevinar*, 2009, 61 (6), pp. 521-531.
- [36] Čaušević, M.; Zehentner, E. Nonlinear seismic analysis of structures according to EN 1998-1:2004. *Građevinar*, 2007, 59 (9), pp. 767-777.
- [37] Golesorkhi, R. et al. *Performance Based Seismic Design for Tall Buildings*. USA: Council on Tall Buildings and Urban Habitat, 2017.
- [38] Brandis, A.; Kraus, I.; Petrovčič, S. Simplified Numerical Analysis of Soil–Structure Systems Subjected to Monotonically Increasing Lateral Load. *Applied Sciences*, 2021, 11 (9), 4219. <https://doi.org/10.3390/app11094219>
- [39] Brandis, A.; Kraus, I.; Petrovčič, S. Nonlinear Static Seismic Analysis and Its Application to Shallow Founded Buildings with Soil-Structure Interaction. *Buildings*, 2022, 12 (11), 2014. <https://doi.org/10.3390/buildings12112014>
- [40] Apostolska, R. et al. Seismic performance of RC high-rise buildings-a case study of 44 storey structure in Skopje (Macedonia). *Technical Gazette*, 2016, 23 (4), pp. 1177-1183. <https://doi.org/10.17559/TV-20150312110020>
- [41] Kostikj I. Nonlinear static analysis of RC building with incorporation of local soil conditions according to EC8. [master thesis], Ss. Cyril and Methodius, Institute of Earthquake Engineering and Engineering Seismology, Skopje, R. Macedonia, 2020.
- [42] Lai C. G.; Martinelli, M. Soil – Structure Interaction. Soil-Structure Interaction Under Earthquake Loading: Theoretical Framework. In: *ALERT Doctoral School 2013, Soil-Structure Interaction*, Kotronis, P.; Tamagnini, C.; Grange, S. (eds.). France: ALERT Geomaterials; 2013, pp. 3-44.
- [43] Bogdanovic, A.; Edip, K.; Stojmanovska, M. Influence of Height in Simulation of Soil Structure Interaction Problems with Dampers. *Selected Scientific Papers - Journal of Civil Engineering*, 2016, 11 (2), pp. 83-92. <https://doi.org/10.1515/sspjce-2016-0021>
- [44] Lagaros, N. D.; Mitropoulou, C. C.; Papadrakakis, M. Time History Seismic Analysis. In: *Encyclopedia of Earthquake Engineering*, Beer, M. et al. (eds.). Berlin, Heidelberg: Springer, 2013, pp. 3751-3767.
- [45] Penelis- G. G.; Papanikolaou, V. K. Nonlinear Static and Dynamic Behavior of a 16-Story Torsionally Sensitive Building Designed According to Eurocodes. *Journal of Earthquake Engineering*, 2010, 14 (5), pp. 706-725. <https://doi.org/10.1080/13632460903308190>
- [46] Mercado-Jaime, A. Seismic Soil-Structure Interaction Effects in Tall Buildings Considering Nonlinear-Inelastic Behaviors. [doctoral thesis], University of Central Florida, 2021.